Inorg. Chem. **2004**, *43*, 155–165

Structure and Physical Properties of [μ-Tris(1,4-bis(tetrazol-1-yl)butane-*N*4,*N*4′)iron(II)] Bis(hexafluorophosphate), a New Fe(II) Spin-Crossover Compound with a Three-Dimensional Threefold Interlocked Crystal Lattice

C. Matthias Grunert, Johannes Schweifer, Peter Weinberger,* and Wolfgang Linert

Institute of Applied Synthetic Chemistry, Vienna University of Technology, Getreidemarkt 9/163-AC, A-1060 Vienna, Austria

Kurt Mereiter

Institute of Chemical Technologies and Analytics, Vienna University of Technology, Getreidemarkt 9/164-SC, A-1060 Vienna, Austria

Gerfried Hilscher, Martin Müller, and Günter Wiesinger

Institute of Solid State Physics, Vienna University of Technology, Wiedner Hauptstrasse 8-10/131, A-1040 Vienna, Austria

Petra J. van Koningsbruggen

Institute of Inorganic and Analytical Chemistry, Johannes-Gutenberg University, Staudingerweg 9, D-55099 Mainz, Germany

Received April 29, 2003

[μ-Tris(1,4-bis(tetrazol-1-yl)butane-*N*4,*N*4′)iron(II)] bis(hexafluorophosphate), $[Fe(btzb)_3](PF_6)_2$, crystallizes in a three-dimensional 3-fold interlocked structure featuring a sharp two-step spin-crossover behavior. The spin conversion takes place between 164 and 182 K showing a discontinuity at about $T_{1/2} = 174$ K and a hysteresis of about 4 K between $T_{1/2}$ and the low-spin state. The spin transition has been independently followed by magnetic susceptibility measurements, ^{57}Fe-Mössbauer spectroscopy, and variable temperature far and midrange FTIR spectroscopy. The title compound crystallizes in the trigonal space group $P\bar{3}$ (No. 147) with a unit cell content of one formula unit plus a small amount of disordered solvent. The lattice parameters were determined by X-ray diffraction at several temperatures between 100 and 300 K. Complete crystal structures were resolved for 9 of these temperatures between 100 (only low spin, LS) and 300 K (only high spin, HS), $Z = 1$ $[Fe(btzb)_3](PF_6)_2$: 300 K (HS), $a = 11.258(6)$ Å, $c = 8.948(6)$ Å, $V = 982.2(10)$ Å^3; 100 K (LS), $a = 10.989(3)$ Å, $c = 8.702(2)$ Å, $V = 910.1(4)$ Å^3. The molecular structure consists of octahedral coordinated iron(II) centers bridged by six *N*4,*N*4′ coordinating bis(tetrazole) ligands to form three 3-dimensional networks. Each of these three networks is symmetry related and interpenetrates each other within a unit cell to form the interlocked structure. The Fe–N bond lengths change between 1.993(1) Å at 100 K in the LS state and 2.193(2) Å at 300 K in the HS state. The nearest Fe separation is along the *c*-axis and identical with the lattice parameter *c*.

Introduction

Spin-crossover materials are increasingly investigated due to their perceived technological importance, with prospects in memory devices and displays.[1] Especially, Fe(II) spin-crossover compounds exhibit favorable response functions toward a change in temperature, pressure, light irradiation (LIESST), and nuclear decay (NIESST)[2]: the thereby occurring interconversion from low-spin (LS; $S = 0$) to high-spin (HS; $S = 2$) state represents the magnetic response, which is frequently associated with a pronounced thermochromic effect. This is, for instance, the case for the extensively studied $[Fe(1\text{-propyl-tetrazole})_6](BF_4)_2$,[2d] where the absorption spectrum is not obscured by ligand- or charge-

* To whom correspondence should be addressed. E-mail: weinberg@mail.zserv.tuwien.ac.at.

(1) Kahn O.; Jay-Martinez, C. *Science* **1998**, *279*, 44.

10.1021/ic034452z CCC: $27.50
Published on Web 12/11/2003

transfer bands, conferring the color arising from the d−d transitions of the Fe(II) ion to the compound, i.e., purple to pink in the LS state and colorless in the HS state. [Fe(1-propyl-tetrazole)$_6$](BF$_4$)$_2$ shows very abrupt spin transitions, a feature which is very well described by the model of elastic interactions[3] and exhibits thermal hysteresis, which is due to a first-order phase transition.[4] Generally, the occurrence of thermal hysteresis in mononuclear Fe(II) spin-crossover compounds may also be brought about by strong intermolecular interactions resulting from the presence of an important hydrogen bonding network[5] or extended $\pi-\pi$ interactions.[6] Unfortunately, these features invoked to be responsible for thermal hysteresis are difficult to control, and hence, alternative strategies involving polynuclear Fe(II) compounds have been applied during the past decade. This quest for polynuclear Fe(II) spin-crossover compounds has been motivated by the consideration that an efficient propagation of the molecular distortions originating from the Fe(II) spin transition through the crystal lattice should be enhanced by the direct covalent intramolecular bonds. This concept has been successfully demonstrated within the series of linear chain compounds of formula [Fe(4-R-trz)$_3$](anion)$_2$·xH$_2$O (4-R-trz = 4-substituted-1,2,4-triazole),[7] where the direct linkage of the Fe(II) spin-crossover centers by triple *N*1,*N*2-1,2,4-triazole bridges was assumed to account for the evident cooperative nature of the spin transition.

Beside one-dimensional polymeric complexes, also 2-D grids and 3-D networks of spin-transition compounds[8] were found to exhibit strong cooperativity, which does not mean that a polymeric structure itself requires strong interactions a priori.[9a] The literature shows that by varying a ligand only slightly the structural and magnetic features of compounds can be effectively influenced. With this strategy on, e.g., iron(II) pyridine complexes, it was already possible to obtain compounds with double[8d] and triple[8e] interlocked grids.

Our strategy of infinitely linked spin-crossover centers is based on the use of α,*β*- and α,*ω*-bis(tetrazol-1-yl)alkane type ligands, which have already been applied to some structurally characterized 1-D, 2-D, and 3-D iron(II) spin-crossover compounds.[9,10] The iron(II) complexes with bridging 1,2-bis(tetrazol-1-yl)alkanes yielded linear chain type coordination polymers with a rather gradual spin-transition behavior which was attributed to a shock-absorber effect induced by the flexible ligand and their column style crystal packing.[9a−c]

Continuing this work, the length of the alkyl spacer has been varied yielding the ligand 1,4-bis(tetrazol-1-yl)butane (abbreviated as btzb) with which the new spin-crossover material [Fe(btzb)$_3$](ClO$_4$)$_2$ has been obtained.[9d] Due to poor crystallinity, only a tentative model of the structure could be worked out which proposed two symmetry-related interpenetrating 3-D [Fe(btzb)$_3$]$^{2+}$ networks.

In this paper, we report on the structure and physical properties of [Fe(*btzb*)$_3$](PF$_6$)$_2$·solv (solv = $^1/_2$MeOH or H$_2$O), a new Fe(II) spin-crossover material consisting of three symmetry-related interlocked 3-D networks. Besides the standard characterization methods for spin-transitions, further insight was gained by variable temperature (VT) far and midrange FTIR spectroscopy.

Experimental Section

General Procedures. Elemental analyses (C, H, and N) were performed by the Mikroanalytisches Laboratorium, Institute for Physical Chemistry, Vienna University, Währingerstrasse 42, A-1090 Vienna, Austria. Thermogravimetry was performed on a Shimadzu TGA-50 analyzer within the temperature range of 25−600 °C at a heating rate of 5 °C min^{-1}. ^{1}H NMR was measured on a Bruker 250 FS FT-NMR spectrometer with deuterated d_6-DMSO. Proton NMR chemical shifts are reported in ppm versus TMS. Midrange FTIR spectra of the ligand and the complex as pellets were recorded within the range 4400−450 cm^{-1} on a Perkin-Elmer 16PC FTIR spectrometer. The ligand was analyzed in a matrix of dry potassium bromide, whereas the complex was used as concentrated sample. Pellets were obtained after pressing the powder of the compounds in vacuo in a hydraulic press for 5 min at a pressure of 12.000 kg/cm^2. Far FTIR spectra were recorded within the range 600−200 cm^{-1} on a Perkin-Elmer System 2000 far FTIR spectrometer. The pure ligand was diluted with polyethylene, whereas the complex was used without further dilution. VT IR spectra in the temperature range 100−303 K were recorded using a Graseby-Specac thermostatable sample holder with polyethylene and silicium windows for the far- and mid-IR ranges, respectively, attached to

(2) (a) König, E. *Prog. Inorg. Chem.* **1987**, *35*, 527. (b) Haasnoot, J. G. *Magnetism: A Supramolecular Function*; Kahn, O., Ed.; Kluwer Academic Publishers: Dordrecht, 1996; p 299. (c) Kahn, O.; Codjovi, E.; Garcia, Y.; van Koningsbruggen, P. J.; Lapouyade, R.; Sommier, L. In *Molecule-Based Magnetic Materials*; Turnbull, M. M., Sugimoto, T., Thompson, L. K., Eds.; ACS Symposium Series 644; American Chemical Society: Washington, DC, 1996; p 298. (d) Gütlich, P.; Hauser, A.; Spiering, H. *Angew. Chem., Int. Ed.* **1994**, *33*, 2024.

(3) (a) Sanner, I.; Meissner, E.; Köppen, H.; Spiering, H. *Chem. Phys.* **1984**, *86*, 227. (b) Spiering, H.; Willenbacher, N. *J. Phys.: Condens. Matter* **1989**, *1*, 10089.

(4) Jung, J.; Schmitt, G.; Wiehl, L.; Hauser, A.; Knorr, K.; Spiering, H.; Gütlich, P. *Z. Phys. B: Condens. Matter* **1996**, *100*, 523.

(5) (a) Sorai, M.; Ensling, J.; Hasselbach, K. M.; Gütlich, P. *Chem. Phys.* **1977**, *20*, 197. (b) Buchen, T.; Gütlich, P.; Sugiyarto, K. H.; Goodwin, H. A. *Chem. Eur. J.* **1996**, *2*, 1134. (c) Sugiyarto, K. H.; Weitner, K.; Craig, D. C.; Goodwin, H. A. *Aust. J. Chem.* **1997**, *50*, 869.

(6) (a) Létard, J. F.; Guionneau, P.; Codjovi, E.; Lavastre, O.; Bravic, G.; Chasseau, D.; Kahn, O. *J. Am. Chem. Soc.* **1997**, *119*, 10861. (b) Létard, J. F.; Guionneau, P.; Rabardel, L.; Howard, J. A. K.; Goeta, A. E.; Chasseau, D.; Kahn, O. *Inorg. Chem.* **1998**, *37*, 4432. (c) Zhong, Z. J.; Tao, J. Q.; Yu, Z.; Dun, C. Y.; Liu, Y. J.; You, X. Z. *J. Chem. Soc., Dalton Trans.* **1998**, 327.

(7) Haasnoot, J. G. *Coord. Chem. Rev.* **2000**, *200−202*, 131.

(8) (a) Real, A. J.; Gaspar A. B.; Niel, V.; Munoz, M. C. *Coord. Chem. Rev.* **2003**, *236*, 121. (b) Vreugdenhill, W.; van Diemen, J. H.; de Graaff, R. A. G.; Haasnoot, J. G.; Reedijk, J. *Polyhedron* **1990**, *9*, 2971. (c) Kitazawa, T. *J. Mater. Chem.* **1996**, *6*, 119. (d) Real, A. J.; Andrés, E.; Muñoz, M. C.; Julve, M.; Granier, T.; Bousseksou, A.; Varret, F. *Science* **1995**, *268*, 165. (e) Moliner, N.; Muñoz, M. C.; Létard, S.; Solans, X.; Meméndez, N.; Goujon, A.; Varret, F.; Real, A. J. *Inorg. Chem.* **2000**, *39*, 5390.

(9) (a) van Koningsbruggen, P. J.; Grunert, M.; Weinberger, P. *Monatsh. Chem.* **2003**, *134* (2), 183. (b) van Koningsbruggen, P. J.; Garcia, Y.; Kahn, O.; Fournès, L.; Kooijman, H.; Haasnoot, J. G.; Moscovici, J.; Provost, K.; Michalowicz, A.; Renz, F.; Gütlich, P. *Inorg. Chem.* **2000**, *39*, 1891. (c) Schweifer, J.; Weinberger, P.; Mereiter, K.; Boca, M.; Reichl, C.; Wiesinger, G.; Hilscher, G.; van Koningsbruggen, P. J.; Kooijman, H.; Grunert, M.; Linert, W. *Inorg. Chim. Acta* **2002**, *339*, 297. (d) van Koningsbruggen, P. J.; Garcia, Y.; Kooijman, H.; Spek, A. L.; Haasnoot, J. G.; Kahn, O.; Linares, J.; Codjovi, E.; Varret, F. *J. Chem. Soc., Dalton Trans.* **2001**, 466.

(10) (a) Bronisz, R. Ph.D. Thesis, University of Wroclaw, Wroclaw, Poland, 1999. (b) Bronisz, R.; Ciunik, Z.; Drabent, K.; Rudolf, M. F. *Conf. Proc., Ital. Phys. Soc.* **1996**, 15−18 (ICAME 1995, Pt. 2).

a Graseby-Specac automatic temperature controller. For the determination of the magnetic susceptibility, the powdered complex was pressed into pellets. VT magnetic susceptibility measurements of the complex were performed with a superconductivity interferometer device (SQUID) in external fields up to 3 T, within the temperature range of 4.2 and 300 K. The data were corrected for temperature independent diamagnetism using Pascal's constants.[11] The ^{57}Fe-Mössbauer spectra were recorded at selected temperatures within 4.2−295 K using a conventional constant acceleration drive system. The source used was ^{57}Co in a Rh-matrix with an activity of about 50 mCi. The data were analyzed using a least-squares fitting program package assuming Lorentzian lines. NaN_3 (99%), triethylorthoformate (99%), glacial acetic acid (99%), 1,4-diaminobutane (>98%), tetrabutylammonium hexafluorophosphate (98%), and NaOH (97%) were obtained from Aldrich, and iron powder (p.a.) from Merck. All other chemicals were standard reagent grade and used as supplied. $FeCl_2 \cdot 4\ H_2O$ was freshly prepared from iron powder and HCl.

1,4-Bis(tetrazol-1-yl)butane (btzb). The synthesis was performed in analogy to the literature.[9d] ^{1}H NMR (250.13 MHz, d_6-DMSO) δ: 1.81 (s, 2H, tz-CH_2−CH_2), 4.50 (s, 2H,tz-CH_2), 9.38 (s, tz-H5), ^{13}C NMR (62.86 MHz, d_6-DMSO) δ: 26.4 (s, tz-CH_2−CH_2), 47.1(s, tz-CH_2), 143.6 (s, tz-C5). Anal. Calcd for $C_6H_{10}N_8$: C, 37.1%; N, 57.7%; H, 5.2%. Found: C, 37.3%; N, 57.1%; H, 5.2%. Mp: 142 °C

[μ-Tris(1,4-bis(tetrazol-1-yl)butane-*N*4,*N*4′)iron(II)] Bis(hexafluorophosphate) Solvate. A 457 mg [2 mmol] portion of tetrabutylammonium-hexafluorophosphate was dissolved in 10 mL of chloroform. A 117 mg [1 mmol] portion of iron(II)chloride tetrahydrate was dissolved in 10 mL of methanol and slowly added to a solution of 583 mg [3 mmol] of btzb in 100 mL of methanol. After stirring for 10 min at room temperature, the solution of tetrabutylammonium-hexafluorophosphate was added to the mixture, which was heated to 40 °C and kept closed at this temperature under moderate stirring for 2 h. Afterward the reaction mixture was kept at room temperature in the dark for 7 days. The product precipitated in the shape of cube-like rhombohedral crystals, which were filtered, washed with ethanol, and dried in vacuo. Yield: 35%. Anal. Calcd for $C_{18}H_{30}FeN_{24}P_2F_{12}$: C, 23.29%; H, 3.257%; N, 36.21%. Found: (powder sample) C, 23.85%; H, 3.02%; N, 35.79%; (crystalline sample) C, 23.86%; H, 2.98%; N, 35.54%. Anal. Calcd taking into account 0.5 methanol per $[Fe(btzb)_3](PF_6)_2$ (for discussion of solvent content see below): C, 23.53%; H, 3.415%; N, 35.60%. Thermogravimetry of the complex showed to be stable up to ∼230 °C. Between ∼230 °C and ∼250 °C, a weight loss of 1−2% corresponding to the suggested solvent content per $[Fe(btzb)_3](PF_6)_2$ was observed (see Figure 1). At about 250 °C a strongly exothermic thermal decomposition was found, which is typical for tetrazole compounds. **WARNING: Tetrazole compounds should be handled with care; they may detonate upon heating or shock**!!!

Crystallographic Studies. A single crystal of $[Fe(btzb)_3](PF_6)_2 \cdot$ solv was glued to a glass fiber and transferred to a Bruker SMART diffractometer (graphite monochromated Mo Kα radiation from a sealed X-ray tube, $\lambda = 0.71073$ Å, platform 3-circle goniometer, CCD area detector, Bruker Kryoflex gas stream cooling device), and unit cell dimensions were measured at 100, 140, 150, 155, 160, 163, 165, 167, 170, 175, 180, 190, 200, and 300 K. Complete sets of diffraction data were collected at $T = 100$, 140, 150, 160, 165, 170, 180, 200, and 300 K. After raw data extraction with program SAINT, absorption and related effects were corrected with program SADABS[12] (multiscan method), and data reduction was carried out with program XPREP.[12] The structure was solved with Patterson and Fourier methods using SHELXS97,[13] and structure refinements on F^2 were carried out with program SHELXL97.[13] Attempts were unsuccessful to find superstructure reflections in the diffraction images at a temperature of about 165 °C where a bump in the temperature versus cell dimension curves was found (Figure 2). Nevertheless, the finding of steps in these curves is of interest

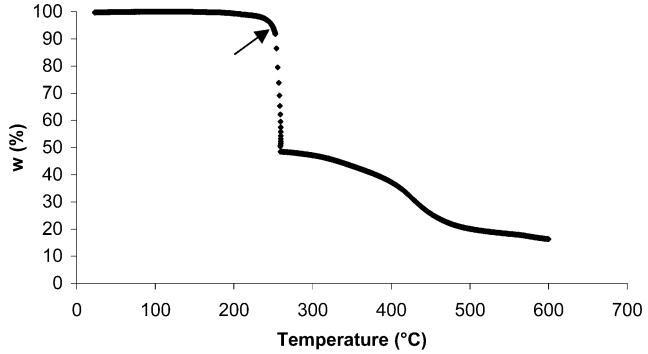

Figure 1. Thermogravimetry of $[Fe(btzb)_3](PF_6)_2 \cdot$solv.

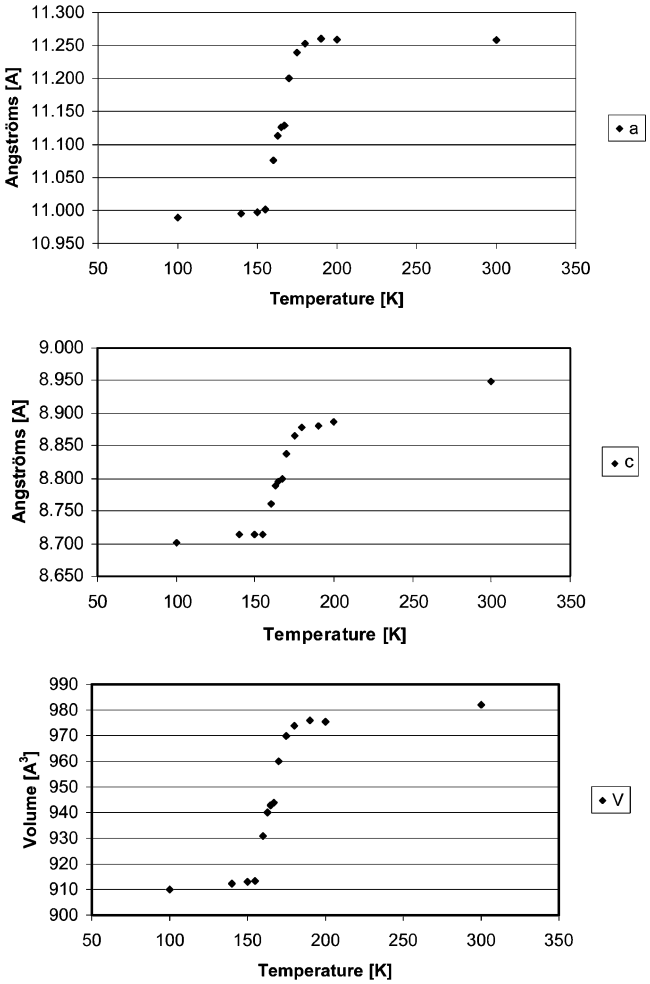

Figure 2. Temperature dependence of the lattice parameters *a*, *c*, and *V*.

(11) Kolthoff, I. M.; Elving, P. J. *Treatise on Analytical Chemistry, Vol. 4*; New York, 1963.

(12) Programs: *SMART*, version 5.054; *SAINT*, version 6.2.9; *SADABS*, version 2.03; *XPREP*, version 5.1; *SHELXTL*, version 5.1; Bruker AXS Inc.: Madison, WI, 2001.

(13) Sheldrick, G. M. *Programs SHELXS97 and SHELXL97*; University of Göttingen: Göttingen, Germany, 1997.

Table 1. Selected Crystallographic Data for $[Fe(btzb)_3](PF_6)_2 \cdot solv$ at 100, 150, 165, 200, and 300 K[a]

	100 K	150 K	165 K	200 K	300 K
a, *b* [Å]	10.989(3)	10.997(8)	11.126(3)	11.259(7)	11.258(6)
c [Å]	8.702(2)	8.714(5)	8.795(3)	8.887(6)	8.948(6)
V [Å^3]	910.1(4)	912.6(11)	942.9(5)	975.6(11)	982.2(10)
reflns collected	13629	7137	4173	7716	14795
reflns unique	1768	1766	1815	1884	1902
params refined	103	103	103	103	111
R1/wR2[b] [$I > 2\sigma(I)$]	0.034/0.071	0.036/0.078	0.044/0.094	0.050/0.128	0.049/0.138
R1/wR2 [all data]	0.035/0.072	0.041/0.080	0.053/0.098	0.053/0.131	0.051/0.142

[a] For all temperatures and without solvent: $C_{18}H_{30}F_{12}FeN_{24}P_2$, $M_r = 949.25$, trigonal, space group $P\bar{3}$ (No. 147), $Z = 1$, $F(000) = 480$, $\mu = 0.62-0.58$ mm^{-1}, $D_x = 1.69-1.62$ g cm^{-3}; rhombohedral crystal of $0.4 \times 0.4 \times 0.3$ mm^3, colorless at 300 K, violet at 100 K; Bruker Smart CCD diffractometer, Mo Kα radiation, $\lambda = 0.71073$ Å. [b] $R1 = \sum||F_o| - |F_c||/\sum|F_o|$, $wR2 = [\sum(w(F_o^2 - F_c^2)^2)/\sum(w(F_o^2)^2)]^{1/2}$.

Table 2. Selected Bond Lengths and Angles for $[Fe(btzb)_3](PF_6)_2 \cdot solv$ at 100, 150, 165, 200, and 300 K with esd's in Parentheses

		100 K	150 K	165 K	200 K	300 K
Fe−N(4)	(6×)	1.9931(11)	1.9971(15)	2.0873(16)	2.1836(18)	2.1932(16)
N(1)−C(1)		1.3328(16)	1.3298(19)	1.325(2)	1.326(2)	1.319(2)
N(1)−N(2)		1.3480(16)	1.347(2)	1.347(2)	1.345(3)	1.334(3)
N(2)−N(3)		1.2963(16)	1.2961(19)	1.289(2)	1.288(3)	1.289(3)
N(3)−N(4)		1.3659(15)	1.3630(18)	1.360(2)	1.359(2)	1.349(2)
N(4)−C(1)		1.3275(16)	1.327(2)	1.323(2)	1.318(2)	1.316(2)
N(1)−C(2)		1.4696(16)	1.471(2)	1.470(2)	1.471(2)	1.470(2)
C(2)−C(3)		1.5263(18)	1.524(2)	1.519(3)	1.512(3)	1.506(3)
C(3)−C(3)		1.533(3)	1.537(3)	1.531(4)	1.525(4)	1.524(4)
P−F(1)	(3×)	1.6071(10)	1.6027(14)	1.5965(15)	1.597(2)	1.591(3)
P−F(2)	(3×)	1.6031(11)	1.5974(15)	1.5881(17)	1.578(2)	1.568(3)
N(4)−Fe−N(4)	(6×)	88.48(4)	88.48(6)	88.28(6)	87.98(7)	88.27(6)
N(4)−Fe−N(4)	(6×)	91.52(4)	91.52(6)	91.72(6)	92.02(7)	91.73(6)
N(4)−Fe−N(4)	(3×)	180.00	180.00	180.00	180.00	180.00

because it parallels with a slight shift the temperature-dependent magnetic behavior of the compound.

For the selected temperatures $T = 100$, 150, 165, 200, and 300 K crystal data as well as details of the data collection and refinement procedure are given in Table 1. Selected bond lengths and angles at these temperatures are given in Table 2. The temperature dependence of the lattice parameters *a*, *c*, and *V* is shown in Figure 2. Further details have been deposited (see Supporting Information available).

Results and Discussion

Structure. The structure of [μ-tris(1,4-bis(tetrazol-1-yl)-butane-*N*4,*N*4′)iron(II)] bis(hexafluorophosphate) was determined at 100, 140, 150, 160, 165, 170, 180, 200, and 300 K. At all these temperatures, the compound crystallizes in the trigonal space group $P\bar{3}$ (No. 147) with cell dimensions which show that there is no phase transition other than a change in the iron spin-state. The asymmetric crystallographic unit comprises an Fe atom in special position 1a ($x, y, z = 0,0,0$), one-half of a btzb ligand in general position 6g (x, y, z) being complemented to the full ligand via duplication by inversion, a noncoordinated PF_6^- unit with P in special position 2d ($^1/_3$, $^2/_3$, z), and finally a cavity around special position 1b ($x, y, z = 0, 0, ^1/_2$) of approximately 80 Å^3 net volume containing minor amounts of disordered solvent (H_2O, CH_3OH), which give rise to a system of symmetry related electron density peaks of low height. At 100 K, the PF_6^- unit is well ordered, which changes above $T_{1/2}$ towards 300 K drastically featuring already considerably disoriented PF_6^- units.

The iron(II) ion is coordinated by six symmetry equivalent tetrazole N(4) atoms in the form of an almost regular FeN_6 octahedron of point symmetry $\bar{3}$ (Table 2). The Fe−N(4) bond lengths at 100 K is 1.9931(11) Å and shows clearly that this is divalent iron in the LS state. The corresponding bond length at 300 K, 2.1932(16) Å, is consistent with divalent iron in the HS state comparable with Gütlich et al.[2d] The change in the linear dimension Fe−N(4) for LS ↔ HS is thus 9.8%. The 1,4-bis(tetrazol-1-yl)butane is centrosymmetric and thus consists of two inversion-related halves with two mutually parallel oriented tetrazole rings linked by a butyl chain with a transoid zigzag configuration. Its bond lengths and bond angles correspond well with related compounds, e.g. 1,6-bis(tetrazol-1-yl)hexane (C. M. Grunert et al., *J. Mol. Struct.*, to be published) but not with the free 1,4-bis(tetrazol-1-yl)butane, which adopts an S-shaped carbon chain in the solid state.[9d] In the title compound, the btzb shows only small changes with temperature, namely an apparent shortening with increasing temperature which stems from the increasing vibrations of the carbon atoms perpendicular to the chain. Due to these vibrations, the mean bond length in the tetrazole ring decreases from 1.334 Å at 100 K to 1.321 Å at 300 K, i.e., by 1.0%. The thermal response of the whole btzb ligand can best be demonstrated by the intramolecular N4−N4′ distance, which decreases from 10.239 Å at 100 K to 10.219 Å at 300 K; this is by 2.0%. In summary, the thermal response of the structure on transition from 100 K to RT is a spin-state dependent expansion of the FeN_6 octahedra by 0.200 Å (Fe−N(4)), whereas the N4−N4′ spacer distance decreases by 0.020 Å, slightly compensating the spin-transition. A point of special interest is the behavior of the structure near 165 K. A bump in the lattice parameter versus temperature curves was found, which parallels a moderate temperature offset of unknown reason on the spectroscopic findings on the compound (see below).

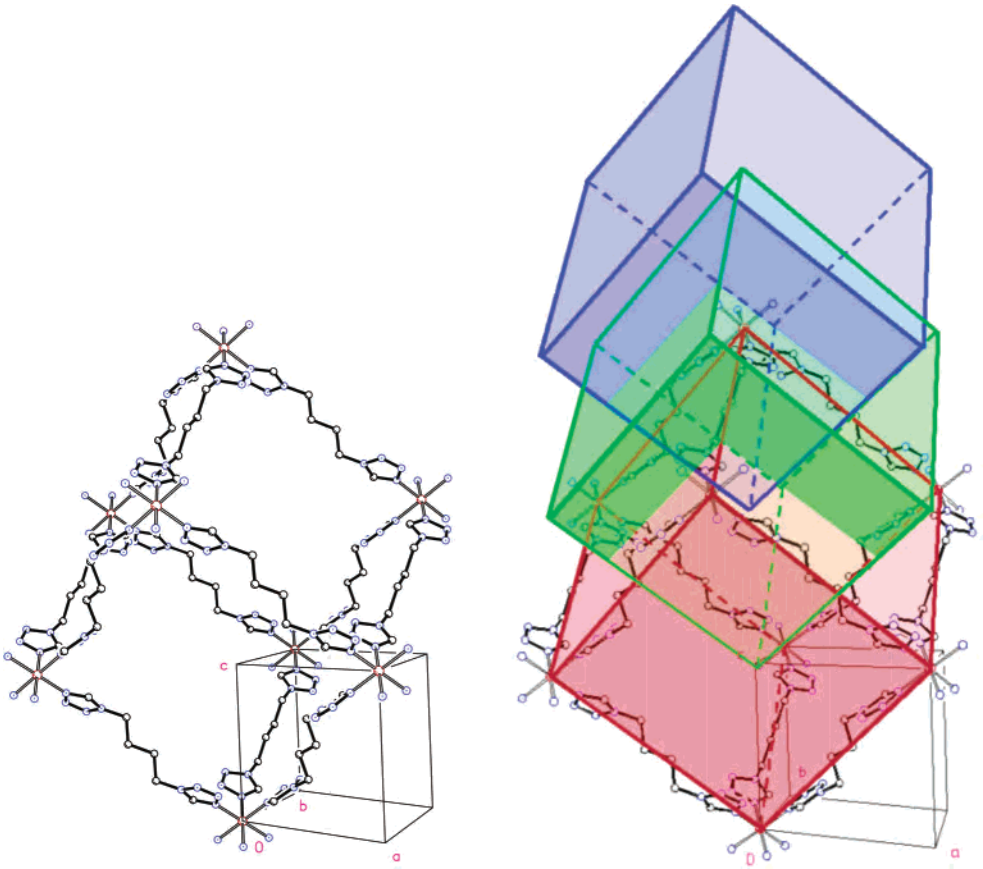

Figure 3. Left: View of one of the three of the 3-dimensional networks of $[Fe(btzb)_3]^{+2}$ and the hexagonal unit cell. Right: Visualization of the three translation-equivalent interpenetrating networks.

This behavior is indicative of some kind of transitional ordering at a temperature where the iron atoms are half in low-spin state and half in high-spin state. Attempts to find changes in diffraction symmetry or superstructure reflections were fruitless, however. Nonetheless, the thermal displacement ellipsoids of the Fe-bound tetrazole nitrogen atom are indicative for the simultaneous presence of high- and low-spin iron in the lattice at 160 and 165 K. At both temperatures, they are notably elongated along the Fe−N bond whereas at higher and lower temperatures they behave clearly more isotropic. Further details on this subject are presented in the Supporting Information.

The 1,4-bis(tetrazol-1-yl)butane ligands link the Fe(II) ions into a 3D framework. This framework or net has Fe atoms at following positions (in terms of *x*, *y*, *z*): 0, 0, 0; 1, 0, 1; 0, 1, 1; −1, −1, 1; 1, 1, 2; 0, −1, 2; −1, 0, 2; and 0, 0, 3 (Figure 3, left). By integer ($n = 0, 1, 2$) translations along the *c*-axis, two further equivalent lattices are formed, which interpenetrate each other but are not mutually linked (Figure 3, right). Only each third repetition along *c* generated identity. Hence, the whole structure is built up by 3 translation equivalent 3-dimensional infinite coordination polymers generating a 3-fold interlocked superlattice. A triple interpenetrating structure of another spin-transition compound is described by Moliner[8e] et al. for two-dimensional grids already. Comparable triply interpenetrating networks without spin-transition properties were recently detected in $KMnAg_3(CN)_6$[14] and a compound based on CMCR.[15] For a more general review of such lattices, the reader is referred to Batten et al.[16]

The PF_6^- anions are located in channel-like spaces at $^1/_3$, $^2/_3$, *z* and $^2/_3$, $^1/_3$, -*z* of the structure (Figure 4, top). Lacking stronger interactions with the cationic framework, the octahedral PF_6^- anion shows increasing thermal motion with increasing temperature and exhibits at room temperature already a significant orientation disorder, which was taken into account in the X-ray structure refinement by introducing two additional partly occupied fluorine sites. Concomitant with these features, the geometry of the PF_6^- octahedron becomes increasingly irregular. See also the Supporting Information regarding 50% ellipsoid plots showing the increasing atomic mobility of the fluorines upon increasing temperature.

At approximately 0, 0, $^1/_2$, there is an open space with a net volume of about 80 Å^3 that is filled by the disordered solvent molecules. They produce an electron density distribution, which was described by three independent partially occupied oxygen sites. Figure 4 (bottom) shows a group of these solvent positions in the unit cell and sketches the other translation equivalent solvent areas by filled ellipsoids. While the solvent content by refinement of 3 partly occupied sites gave a solvent content of 1.3 O atoms per formula unit, an

(14) Geiser, U.; Schlueter, J. A. *Acta Crystallogr.* **2003**, *C59* (21−23).
(15) Ma, B. Q.; Coppens, P.; *Chem. Commun.* **2003**, 412.
(16) Batten, S. R.; Robson, R. *Angew. Chem.* **1998**, *110*, 1558.

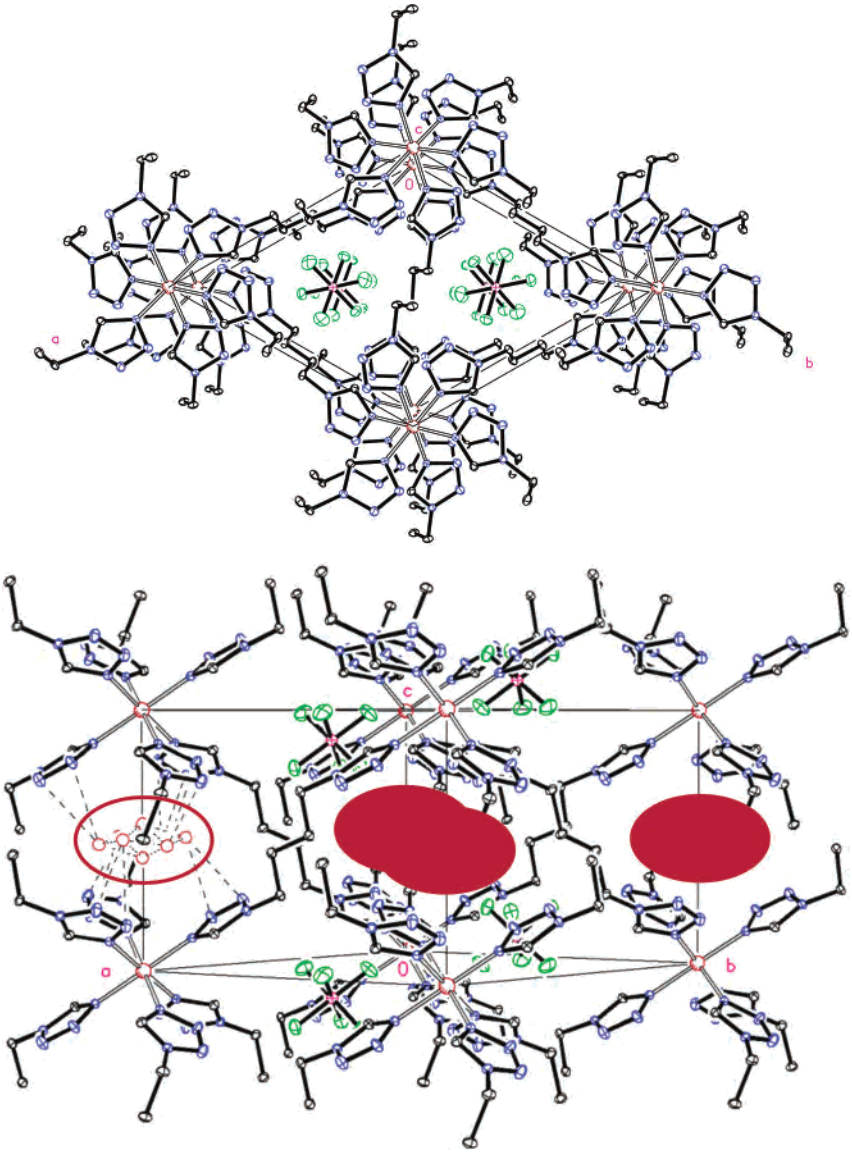

Figure 4. $[Fe(btzb)_3](PF_6)_2$·solv seen along the *c* axis (top), and approximately along [110] (bottom) showing one cavity filled by solvent molecules and sketching the other positions for solvent molecules between the unit cell.

alternative structure refinement using procedure squeeze of program PLATON gave a scattering density electron count of 10 electrons per cavity, in good agreement with the previous occupation. Thus, both approaches show clearly that there is some solvent in the cavity. Since these solvent molecules see essentially π-electron clouds of the tetrazole rings plus some butane-chain hydrogen atoms, the solvent appears to be included unspecifically and serves only to fill open spaces which the 3 interpenetrating 3-dimensional lattices leave open.

^{57}Fe-Mössbauer spectroscopy. The spectra of the powder sample of $[Fe(btzb)_3](PF_6)_2$·solv were recorded at ambient temperature, at liquid helium temperature, and at temperatures around the high-spin ↔ low-spin transition (displayed in Figure 5).

As is evidenced from the subspectra between $T = 4.2$ K and $T = 200$ K, our compound shows a complete spin transition. The subspectra measured around the $T_{1/2} \sim 175$ K indicate a two-step spin transition as well as a small thermal hysteresis for the low temperature step (see Table 3 and Figure 6 right), which was independently proven by VT SQUID measurements.

Magnetic Studies. The magnetic behavior of $[Fe(btzb)_3](PF_6)_2$·solv is shown in Figure 6 (left) in the form of a $\chi_M T$ versus T plot, which was calculated from the magnetization M. Using eq 1, the molar ratio of high-spin and low-spin species γ_{HS} depending on T can be derived (Figure 6, right). The value of about 0.1 cm^3 K/mol at 150 K after diamagnetic correction[11] was taken as $\gamma_{HS} = 0$ in accordance with the ^{57}Fe-Mössbauer data. The residue magnetization might be caused by a small amount of iron(III), which was too small to be detected by ^{57}Fe-Mössbauer spectroscopy. The SQUID measurements have been performed in fields up to 3 T yielding a good scaling of the susceptibility.

$$\gamma_{HS} = [(\chi T) - (\chi T)_{LS}]/[(\chi T)_{HS} - (\chi T)_{LS}] \qquad (1)$$

Upon cooling from room temperature, this ratio remains constant to ~200 K. Between ~200 and ~184 K, γ_{HS} only

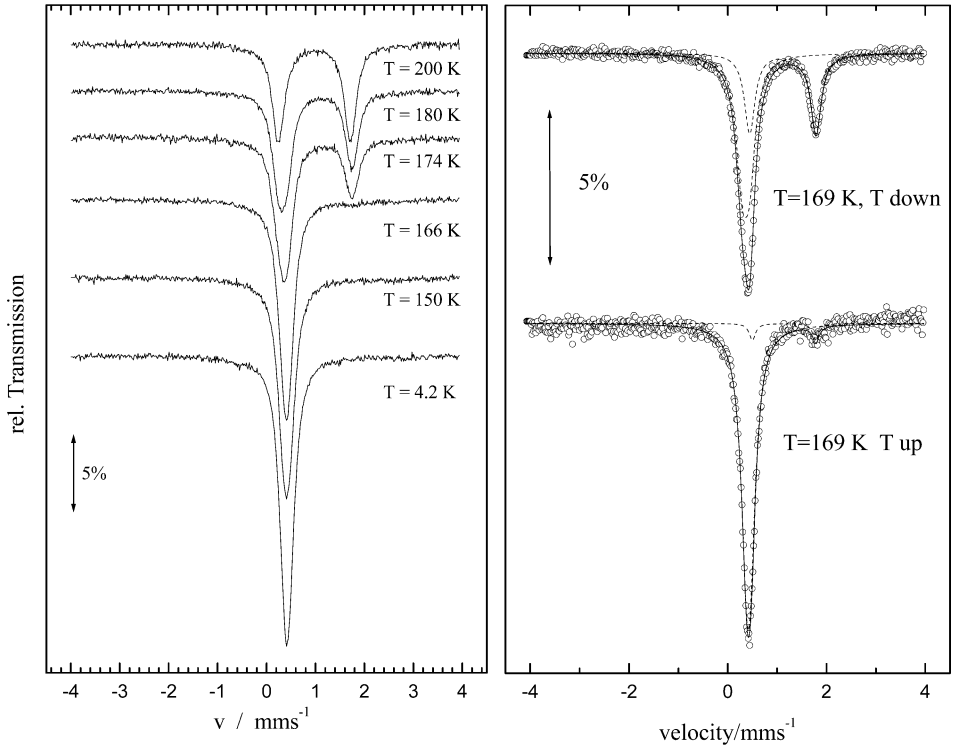

Figure 5. ^{57}Fe-Mössbauer spectra of $[Fe(btzb)_3](PF_6)_2$·solv at selected temperatures

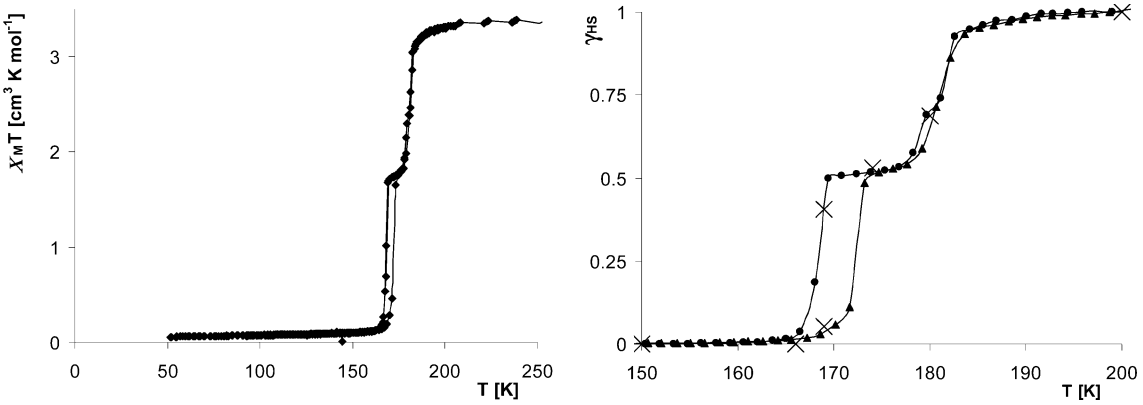

Figure 6. $\chi_M T$ vs T (left) and γ_{HS} vs T (● cooling; and ▲ heating) and ^{57}Fe-Mössbauer spectroscopy (×) (right) shows a two-step spin transition with hysteresis for the part $\gamma_{HS} < 0.5$.

Table 3. Isomer Shift (δ) and Quadrupole Splitting (Δ) Obtained for $[Fe(btzb)_3](PF_6)_2$

T (K)	A_{LS} (%)	δ(LS) (mm s^{-1})	Δ(LS) (mm s^{-1})	A_{HS} (%)	δ(HS) (mm s^{-1})	Δ(HS) (mm s^{-1})
4.2	100.0	0.417	0.097	0.0		
150	100.0	0.409	0.122	0.0		
166	100.0	0.405	0.104	0.0		
169[a]	94.7	0.416	0.070	5.3	1.140	1.285
169[b]	59.4	0.361	0.148	40.6	1.115	1.342
174	46.9	0.404	0.101	53.1	0.992	1.512
180	31.4	0.403	0.099	68.6	0.989	1.516
200	0.0			100.0	0.978	1.471

[a] Heating. [b] Cooling.

gradually decreases approximately 10%, featuring a sharp change to $\gamma_{HS} \sim 0.5$ between $T \sim 184$ K and $T \sim 177$ K in a first step. Both by magnetic measurements and by ^{57}Fe-Mössbauer experiments, $T_{1/2} \sim 174$ K was found. The second step of the spin transition between $T \sim 169$ K and $T \sim 165$ K shows a small thermal hysteresis of ~4 K. Upon heating, this second spin transition step occurs between 168 and 174 K. For $T < 165$ K, the ratio γ_{HS} reaches a value of less than 0.05 (see Figure 6, right).

VT FTIR Spectroscopy. Variable temperature IR spectroscopy and far IR spectroscopy are well-known techniques to give an additional proof of the spin transition behavior.[17] In the spectra of the free ligand and the iron(II) hexafluorophosphate complex, several characteristic bands for the tetrazole ring as well as for the alkyl chain were identified. Figure 7 gives a comparison of these spectra. Because not every band of the complex is sufficiently sensitive to observe the spin-transition behavior, not all occurring bands have been looked for in detail. A detailed assignment of the

(17) (a) Müller, E. W.; Ensling, J.; Spiering, H.; Gütlich, P. *Inorg. Chem.* **1983**, *22*, 2074. (b) Herber, H. R. *Inorg. Chem.* **1987**, *26*, 173−178. (c) Stassen, A. F.; Grunert, M.; Dova, E.; Schenk, H.; Wiesinger, G.; Müller, M.; Weinberger, P.; Linert, W.; Haasnoot, J. G.; Reedijk, J. *Eur. J. Inorg. Chem.*, **2003**, 2273.

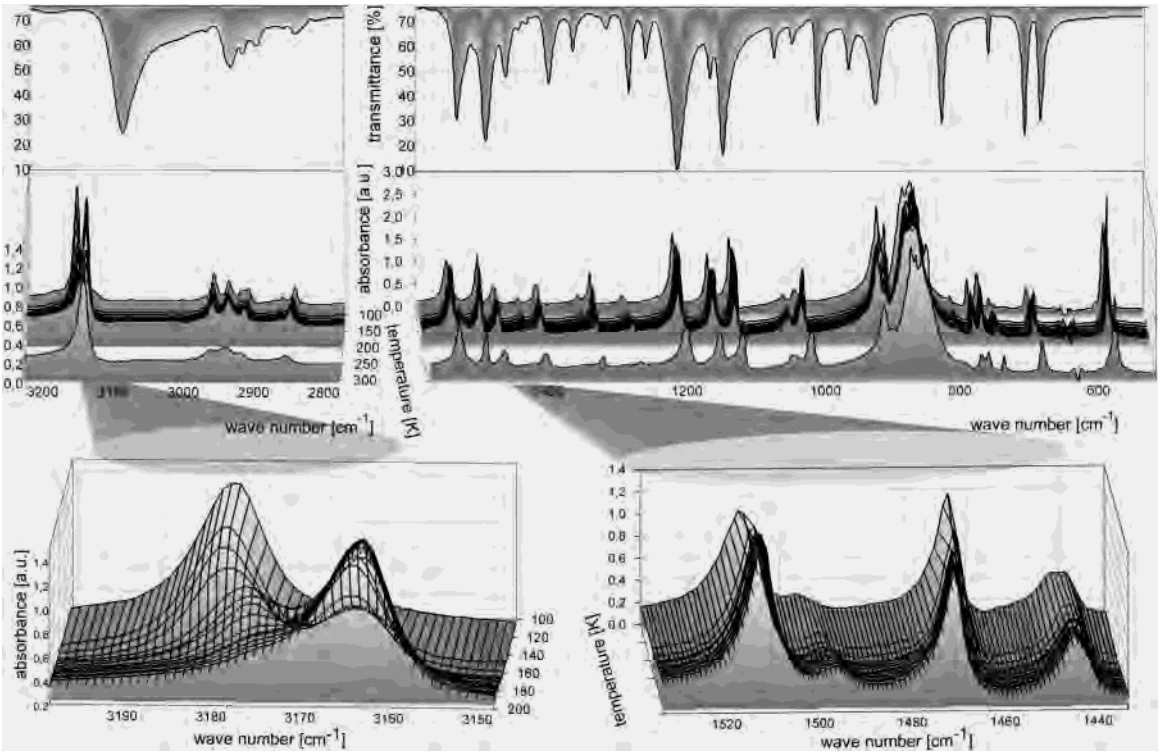

Figure 7. Comparison of the free ligand (btzb) (top), with its iron(II) hexafluorophosphate complex, measured at several temperatures between 303 and 103 K (middle) and the focus on the bands ν_{C-H} (bottom, left) and $\nu(N_2{=}N_3)$ and δ_{CH2}.

Table 4. Prominent Mid- and Far-IR Bands of the Ligand btzb and Its Iron(II) Hexafluorophosphate Complex[a]

	btzb	$[Fe(btzb)_6](PF_6)_2$ HS at 303 K	$[Fe(btzb)_6](PF_6)_2$ LS at103 K
ν(C−H)	3317s	3165vs	3181vs
ν(C−H)	2962m, 2945w, 2925w, 2879vw	2985m, 2963m, 2938m, 2876w	2986m, 2965m, 2889w, 2871w
aromatic overtone band	1768w	1773w	1748w
$\nu(N_2{=}N_3)$ $\{+\nu(C_5{-}N_1) + \nu(C_{alkyl}{-}N_1)\}$	1492s	1506vs	1485s
$\delta(C{-}H_2)$	1450s, 1422m	1468s, 1441m	1464s, 1441m
$\nu(N_1{-}C_{alkyl})$	1359m	1381m	1378m
$\delta(ring_1)$	1243m	1243w	1253m
$\nu(C{=}N_4)$, $\nu(N_1{-}N_2)$	1173vs	1178vs	1180vs
ν(C−N), δ(C−H)	1107s	1096s	1099s
$\nu(N_3{-}N_4)$	1033w	1020m	1020m
$\nu(N_1{-}N_2)$	973sh	971s	970s
$\delta(ring_2)$ in plane bending $\{\delta(NCN)\}$	970s	997s	1005m
$\delta(ring_3)$ in plane bending $\{\delta(NNN)\}$	876m	891vs	885vs
$\nu(P{-}F)$[10]		∼841s	∼836s
$\delta(C{-}H_2)$	723m	718m	723w
$\gamma(ring_4)$ out of plane	670s, 647s	662s	668s
$\delta(P{-}F)$[10]		557vs	558vs
$\delta(ligand_1)$	432vs	453s	460s
$\nu(LS_1)$		(415vw)	412s
$\nu(LS_2)$		(397vw)	392w
$\nu(HS_1)$, $\nu(LS_3)$		359m	346s
$\delta(ligand_2)$	349m		

[a] Frequencies in cm^{-1}: ν, stretching; δ, deformation or in-plane vibration of the ring; γ, out-of-plane.

vibrations has been done for 0-dimensional iron(II) complexes with 1-(2-halogenethyl)tetrazoles in a recent work by Stassen et al.[17c] Table 4 lists the most prominent bands for the free ligand btzb and its complex in the LS and HS state in the mid- and far-IR ranges.

In the 0-dimensional hexakis[1-(2-halogenethyl)tetrazole] iron(II) tetrafluoroborate complexes,[17c] the aromatic C−H stretching vibration does not shift very significant upon spin transition, whereas the ring vibrations and the $-CH_2$ deformation bands change notably. In contrast to these mononuclear compounds, our 3-dimensional network complex shows shifts of about 16 cm^{-1} for the vibrations of the aromatic hydrogen, whereas the effect of spin conversion on individual stretching vibrations in the tetrazole ring itself is marginal (see Figure 7, bottom). Only an aromatic breathing mode (δ_{ring1}) and a more or less broad aromatic overtone band are significantly affected. Therefore, the focus of interest in our case is the single aromatic C−H bond of the tetrazole ring, which does not couple with any other vibrational modes. Upon spin transition of the iron(II), the bond strengths of the nearest neighbor bonds and, to a lesser extent but still detectable, of the next-nearest neighbor bonds

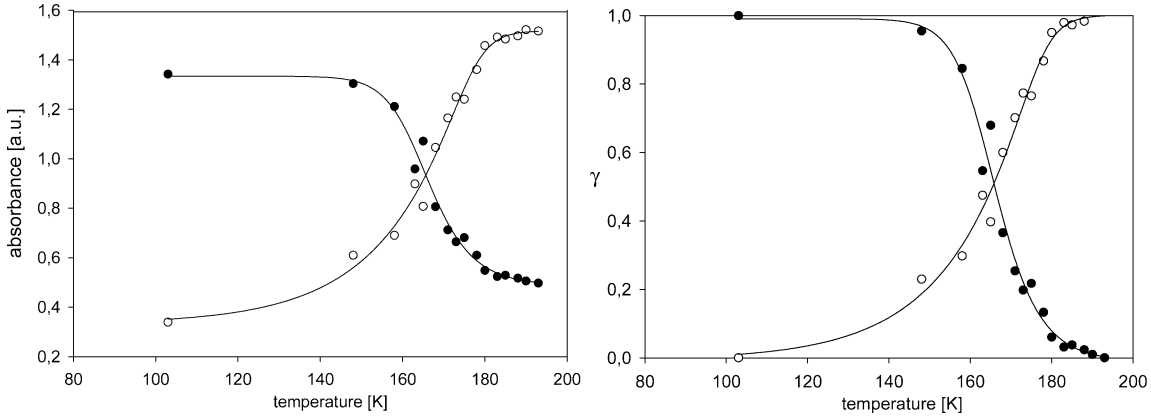

Figure 8. Absorbance vs temperature of the ν_{C-H} HS (○) and LS (●) (left); ratio (γ) for the spin state with γ: $= \gamma_{HS}$ (○) and γ: $= \gamma_{LS}$ (●) (right). The lines are meant to guide the eyes.

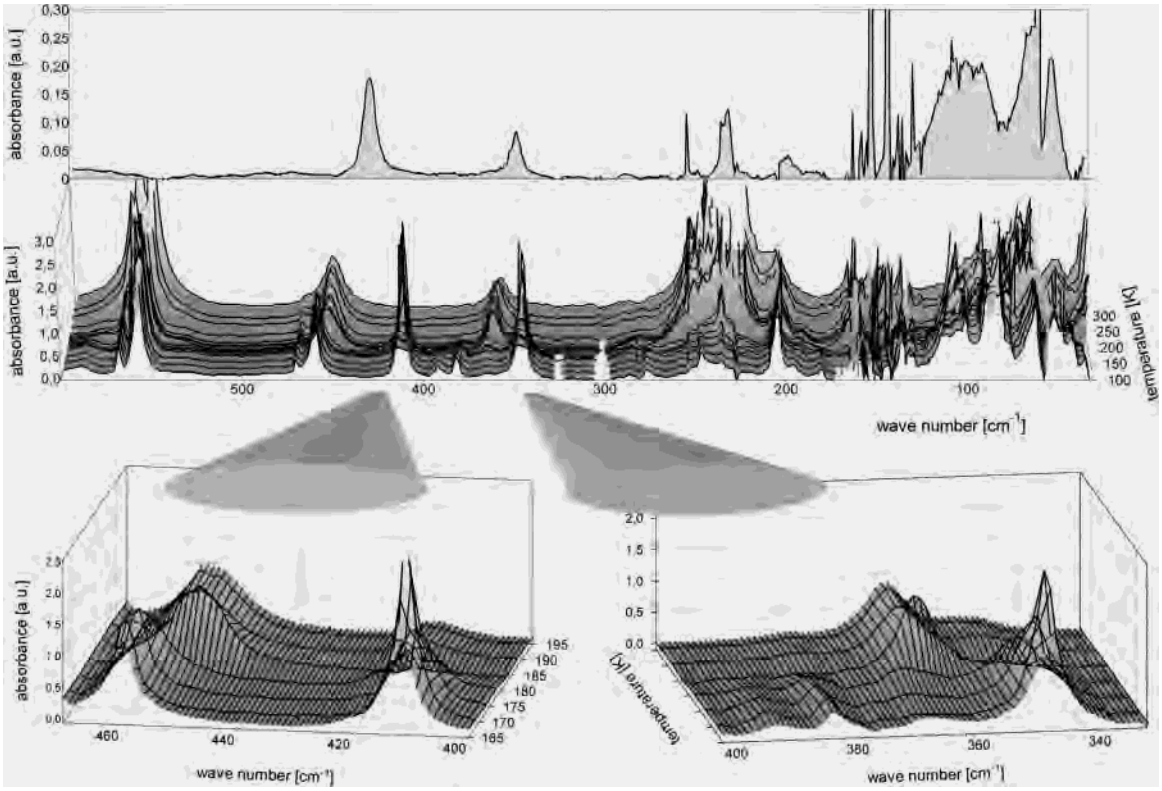

Figure 9. Far-IR spectra of the free ligand (btzb) at room temperature (top), with its iron(II) hexafluorophosphate complex, measured at different temperatures between 298 and 103 K (middle), and the focus on several bands of the complex, which are changing due to the spin conversion (bottom).

change yielding a shift of the very sharp and strong band assigned to this ν_{C-H} stretching vibration. Figure 8 represents the peak intensity of the HS and LS bands and the calculated ratio γ of HS and LS species. $T_{1/2}$ is estimated to 167 K, which is comparable with the temperature dependence of structural data (see lattice parameters vs T in Figure 2) but a slightly lower value than calculated from magnetic and ^{57}Fe-Mössbauer measurements. This difference originates mainly from the somehow arbitrary definition of a baseline for the peak intensity determination, and is additionally affected by the slight band overlapping and might be due to the temporary pressure treatment during the sample preparation.[18] Thus, variable temperature midrange FTIR spectroscopy supports the data obtained by magnetic measurements qualitatively and yields an independent proof of the coexistence of high-spin and low-spin species around $T_{1/2}$.

The far FTIR spectra (see Figure 9), apart from a broadening absorption at 562 cm^{-1} attributable to vibrations within the PF_6^- anion, show intraligand deformation bands (e.g., $\delta_{ligand1}$), which shift upon coordination (see Table 4). These bands are affected by the thermal spin conversion of the iron(II) and, therefore, feature a smooth and gradual shifting of about 7 cm^{-1}. In contrast, those bands attributed to metal-to-ligand vibrations are vanishing and occurring

(18) (a) Haddad, M. S.; Federer, W. D.; Lynch, M. W.; Hendrickson, D. N. *J. Am. Chem. Soc.* **1980**, *102*, 1468. (b) Müller, E. W.; Spiering, H.; Gütlich, P. *Inorg. Chem.* **1984**, *23*, 119. (c) Ksenofontov, V.; Spiering, H.; Schreiner, A.; Levchenko, G.; Goodwin, H. A.; Gütlich, P. *J. Phys. Chem. Solids* **1999**, *60*, 393.

according to the HS ↔ LS ratio {e.g., ν_{Fe-N}(HS) and ν_{Fe-N}(LS)}. Thus, the parallel existence of the bands for the ν_{Fe-N}(HS) and ν_{Fe-N}(LS) around the $T_{1/2}$ are a further independent proof for the coexistence of both species (see Figure 9). LS bands (412 cm^{-1}, 392 cm^{-1}, 346 cm^{-1}, and 345 cm^{-1}) and the HS band (359 cm^{-1}) show clearly the spin transition about 180 K, which is close to what can be observed via magnetic experiments. The region around 230 cm^{-1} contains a multitude of overlapping bands, belonging to deformations of the whole ligand and the octahedral surrounded iron(II). These bands are well influenced by the spin transition, but the strong overlapping prevents a more detailed interpretation.

Conclusion

In contrast to the tentatively solved structure of $[Fe(btzb)_3](ClO_4)_2$,[9d] the title compound $[Fe(btzb)_3](PF_6)_2$·solv is an analogue Fe(II) spin-crossover compound with a proven X-ray structure of a 3-fold interlocked three-dimensional lattice with spin-transition properties. The structure was determined for the pure low-spin as well as for the pure high-spin species as well as at various temperatures within the range of the spin transition. Our compound features a supramolecular catenane structure consisting of three interlocked 3-D networks exhibiting a complete spin transition, which is accompanied by a pronounced thermochromic effect. This is independently evidenced by ^{57}Fe-Moessbauer, magnetic studies, X-ray diffraction, and FTIR spectroscopy.

In the complexes of 1,2-bis(tetrazole-1-yl)alkane ligands,[9a−c] a gradual spin-transition behavior is observed, because the one-dimensional chain type coordination polymers lack a strong cooperative effect due to the flexible bridging ligand (shock absorber effect[9a]). The elongation of this type of ligands should yield even worse cooperativity between neighboring centers. Additionally, one should expect a lower degree of cooperativity as the spin state changing iron centers get further apart, with the consequence that changes in the phonon system and elastic interactions due to the spin transition can be communicated less effectively to nearby iron centers rather than closer distant ones. However, the present work shows that the crucial point is the 3-D packing of the whole coordination polymer and not the rigidity of the ligand itself. Due to the perfect size ratio of the PF_6^- filling the cavities in the structure and the bridging ligand btzb, the packing density of the compound due to the 3-fold interlocked system suppresses distortions and twisting of the per se very flexible ligand due to the simple lack of space.

The comparison with the tentative model of the structure $[Fe(btzb)_3](ClO_4)_2$[9d] indicates that the small change in the size of the anions seems to play a predominant role, possibly as a template, for an optimal packing and in determining the number of $[Fe(btzb)_3]^{2+}$ lattices that are interlocked. Our compound comprises a highly symmetric space group where all iron atoms and all ligands are equivalent, which is not the case for $[Fe(btzb)_3](ClO_4)_2$.[9d] In the latter case, two of the six ligands are arranged in the *syn*- instead of the *anti*-conformation. This already points out that the dimensions and conformation of the building blocks constituting the 3-D catenane network of our compound are excellently fitting together and resulting in the good quality of the crystals, which is a very surprising feature of this substance.

A convincing proof for this has been recently found by us in the $[Cu(btzb)_3](ClO_4)_2$ equivalent, which shows topologically the same type of triply interwoven lattice but is collapsed in comparison to the title compound and shows therefore monoclinic symmetry.

Another point to discuss is the fact of a two-step spin transition occurring at $\gamma_{HS} = 0.5$ leading to the obvious question whether there are two slightly different iron(II) sites such as the two crystallographically nonequivalent iron(II) sites in $[Fe(btr)_3](ClO_4)_2$.[19] But according to the crystallographic structure data as well as to ^{57}Fe-Mössbauer data, only one iron(II) site is present. This gives rise to another explanation for this phenomenon. We assume the thermodynamic stabilization of an alternating ordering of the HS and the LS iron(II) sites around $T_{1/2}$ being the reason for that. This point of view is supported by a theoretical model, developed by A. B. Koudriavtsev et al.,[20] based on ideas of H. Köppen et al.[21] In the case of a series of mononuclear halogenated ethyltetrazol iron(II) complexes, this model was already applied successfully to explain the spin transition behavior.[22a,b] Unfortunately, a long-range ordering of such a proposed alternating HS−LS− arrangement at $T_{1/2}$ causing the discontinuity of the spin transition curve was not detectable by X-ray diffraction; i.e., no superstructure was found. However, the notable elongation of the displacement ellipsoids of the Fe-bound tetrazole nitrogen atoms at $T =$ 165 K (i.e., at the discontinuity of the spin transition) shows at least that the Fe−N mean bond lengths at this temperature result from a superposition of two distinct spin states in one crystallographic position. The absence of detectable superstructure reflections has then to be interpreted that HS−LS ordering domains are comparatively small. But at least the lattice parameter discontinuity at ca. 165 K is a clue for this ordering. For a graphical representation of the change of the displacement ellipsoids, see Figure S2 of the Supporting Information.

Furthermore, our compound features an unexpected abrupt spin transition despite the rather large Fe···Fe separation, which proves again that the predominant factor guiding the abruptness of the spin transition is not really the rigidity of the ligand itself, but rather the overall stiffness of the whole crystal lattice depending on the density and perfect crystal packing.

Further comparisons may be made with the first supramolecular 2-D catenane $[Fe(tvp)_2(NCS)_2]$·CH_3OH (tvp = 1,2-di-(4-pyridyl)-ethylene) exhibiting thermal spin-crossover

(19) Garcia, Y.; Kahn, O.; Rabardel, L.; Chansou, B.; Salmon L.; Tuchagues, J.-P. *Inorg. Chem.* **1999**, *38*, 4663.
(20) Koudriavtsev A. B.; Jameson, R. F.; Linert, W. *The Law of Mass Action*; Springer-Verlag: New York, 2000; Chapter 7.
(21) Köppen, H.; Müller, E. W.; Köhler, C. P.; Spiering, H.; Meissner, E.; Gütlich, P. *Chem. Phys. Lett.* **1982**, *91*, 348.
(22) (a) Koudriavtsev, A. B.; Stassen, A. F.; Haasnoot, J. G.; Grunert, M.; Weinberger, P.; Linert, W. *Phys. Chem. Chem. Phys.* **2003**, *5*, 3666−3675. (b) Koudriavtsev, A. B.; Stassen, A. F.; Haasnoot, J. G.; Grunert, M.; Weinberger, P.; Linert, W. *Phys. Chem. Chem. Phys.* **2003**, *5*, 3676−3683.

behavior.[23] The Fe···Fe separation through the tvp ligand is 13.66 Å. The Fe···Fe separations involving metal ions originating from different interpenetrating layers are 22.59 and 15.36 Å. The difference in ligand dimensions between tvp and btzb leads to a somewhat larger Fe···Fe separation over the direct btzb linkage, i.e., 14.35 Å. However, the interweaving of three 3-D lattices gives rise to extremely short Fe···Fe separations of 8.84 Å between symmetry related nonconnected lattices. This short iron−iron separation is in the same order of magnitude as in the $[Fe(btr)_3](ClO_4)_2$ (btr = 4,4′-bis-1,2,4-triazole).[19] This is despite the fact that this short iron−iron separation is found in the triazole compound along the chains whereas between neighboring networks of $[Fe(btzb)_3](PF_6)_2$·solv this distance alone turns out to be not among the important factors for an abrupt spin transition.

The VT FTIR study for $[Fe(btzb)_3](PF_6)_2$·solv has demonstrated for the first time quantitatively that a spin transition can be detected from changes in the tetrazole vibrations. Although IR spectroscopy has been frequently applied for monitoring Fe(II) spin-crossover behavior, its use has up to now been limited to follow the change of vibrational frequencies originating from atoms in the direct vicinity of the Fe(II) spin-crossover center, such as monitoring changes in the far-infrared, i.e., the ν_{Fe-N}(ligand) vibrations,[24] or by focusing on the ν_{C-N} stretching vibration originating from coordinated co-ligands NCX^- (X = S, Se)[25] or $[TNCQ]^-$ [26] units.

Our study clearly showed that the frequency and position of the observed ligand vibration (i.e., the C−H stretching vibration of the single aromatic tetrazole carbon atom) is altered upon the change in the electronic structure (i.e., population or depopulation of the antibonding e_g-orbital of the iron(II) center) associated with the spin-transition. Therefore, the spin-transition temperature ($T_{1/2}$) can be determined from the VT infrared data via quantification of the intensity of the bands associated with the ν_{C-H} stretching vibration of the $[Fe(btzb)_3](PF_6)_2$·solv in HS or LS state. Due to the fact that this vibrational mode is practically not coupling with any other vibrational modes, the γ_{HS} versus T curve derived from the intensity of the ν_{C-H} stretching vibration yielded a $T_{1/2} \sim 167$ K, which is in quite reasonable agreement with the $T_{1/2} \sim 174$ K obtained from the VT magnetic susceptibility measurements or ^{57}Fe-Mössbauer spectroscopy. Additionally, the IR spectra are further direct proof of the coexistence of both LS and HS Fe(II) ions around the spin-transition temperature, $T_{1/2}$.

Ongoing research on this type of polytetrazole systems is currently being carried out. Variation of the length of the α,ω-bis(tetrazole-1-yl)alkane linker in combination with a variation of anion size provides a solid basis for tuning the spin-crossover behavior by modifying the nature of the linkage, and thereby allowing a systematic tuning of the crystal packing. A fascinating playground for the construction of supramolecular architectures is the size of the 3D network, thus opening an intriguing chance of extending the size and maybe the number of independent interwoven networks.

Acknowledgment. Thanks for financial support are due to the "Fonds zur Förderung der Wissenschaftlichen Forschung in Österreich" (Project 15874-N03), to the Training and Mobility of Researchers Network (TMR) project "Thermal and Optical Spin State Switching" (TOSS) supported by the European Community under Contract ERB-FMRX-CT98-0199, and to the European Science Foundation under the project "Molecular Magnets".

Supporting Information Available: Tables and figures giving crystallographic details for the temperature-dependent structure analysis of the title compound, and a set of crystallographic files in CIF format for each temperature. Set of figures showing the 50% ellipsoids for several temperatures illustrating the changes in atomic mobility. Three photographic snapshots of the single crystal showing the thermochromic behavior at $T = 150$ K (deep purple color, pure LS), $T = 170$ K (pink color, around $T_{1/2}$), and $T = 200$ K (colorless, pure HS). This material is available free of charge via the Internet at http://pubs.acs.org.

IC034452Z

(23) Real, J. A.; Andrés, E.; Munoz, M. C.; Julve, M.; Granier, T.; Bousseksou, A.; Varret, F. *Science* **1995**, *268*, 265.
(24) (a) Hutchinson, B.; Daniels, L.; Henderson, E.; Neill, P. *J. Chem. Soc., Chem. Commun*. **1979**, 1003. (b) Müller, E. W.; Ensling, J.; Spiering, H.; Gütlich, P. *Inorg. Chem*. **1983**, *22*, 2074.
(25) (a) Baker, W. A., Jr.; Long, G. J. *J. Chem. Soc., Chem. Commun*. **1965**, *15*, 368. (b) König, E.; Madeja, K. *Inorg. Chem*. **1967**, *6* 48. (c) König, E.; Madeja, K. *Spectrochim. Acta* **1967**, *23A*, 45. (d) Zilverentant, C. L.; van Albada, G. A.; Bousseksou, A.; Haasnoot, J. G.; Reedijk, J. *Inorg. Chim. Acta* **2000**, *303*, 287.
(26) Kunkeler, P. J.; van Koningsbruggen, P. J.; Cornelissen, J. P.; van der Kraan, A. M.; Spek, A. L.; Haasnoot, J. G.; Reedijk, J. *J. Am. Chem. Soc*. **1996**, *118*, 2190.